Development of a Bio-Based Composite Material from Soybean Oil and Keratin Fibers

Chang K. Hong, Richard P. Wool

Department of Chemical Engineering and Center for Composite Materials, University of Delaware, Newark, Delaware 19716

Received 27 June 2004; accepted 28 May 2004
DOI 10.1002/app.21044
Published online in Wiley InterScience (www.interscience.wiley.com).

ABSTRACT: A novel bio-based composite material, suitable for electronic as well as automotive and aeronautical applications, was developed from soybean oils and keratin feather fibers (KF). This environmentally friendly, low-cost composite can be a substitute for petroleum-based composite materials. Keratin fibers are a hollow, light, and tough material and are compatible with several soybean (S) resins, such as acrylated epoxidized soybean oil (AESO). The new KFS lightweight composites have a density $\rho \approx 1$ g/cm^3, when the KF volume fraction is 30%. The hollow keratin fibers were not filled by resin infusion and the composite retained a significant volume of air in the hollow structure of the fibers. Due to the retained air, the dielectric constant, *k*, of the composite material was in the range of 1.7–2.7, depending on the fiber volume fraction, and these values are significantly lower than the conventional silicon dioxide or epoxy, or polymer dielectric insulators. The coefficient of thermal expansion (CTE) of the 30 wt % composite was 67.4 ppm/°C; this value is low enough for electronic application and similar to the value of silicon materials or polyimides used in printed circuit boards. The water absorption of the AESO polymer was 0.5 wt % at equilibrium and the diffusion coefficient in the KFS composites was dependent on the keratin fiber content. The incorporation of keratin fibers in the soy oil polymer enhanced the mechanical properties such as storage modulus, fracture toughness, and flexural properties, ca. 100% increase at 30 vol %. The fracture energy of a single keratin fiber in the composite was determined to be about 3 kJ/m^2 with a fracture stress of about 100–200 MPa. Considerable improvements in the KFS composite properties should be possible by optimization of the resin structure and fiber selection. J Appl Polym Sci 95: 1524–1538, 2005

Key words: bio-based composite materials; soybean oils; keratin fibers; low density; dielectric properties; chicken feathers

INTRODUCTION

The development of affordable composite materials from renewable sources, such as plant oils and keratin feather fibers, offers both economic and environmental advantages.[1–7] The use of renewable materials contributes to global sustainability and the diminution of global warming gases. As the number of applications of composite materials continues to increase, an alternative source of petroleum-based composites becomes important. Soybean oils and keratin avian feather fibers (KF) are found in abundance in all parts of the world, potentially making them ideal alternatives for petroleum-based materials, subject to suitable technology development. It has been shown that the resins from soybean oil can be a substitute for liquid molding resins, such as unsaturated polyester resins, vinyl esters, and epoxy resins.[1,3,5] The keratin fiber is also a possible replacement for synthetic reinforcing fibers.[8,9]

Soybean resins are based on triglycerides, which are the major component of plant and animal oils. Triglycerides are composed of three fatty acids joined at a glycerol juncture.[10] Although unmodified triglycerides do not readily polymerize, the chemical functionality necessary to cause polymerization can be easily added to the triglycerides. The active sites on the modified triglycerides can be used to introduce polymerizable groups, using the same synthetic techniques that have been applied in the synthesis of petrochemical-based polymers.[1,3,5–7] With suitable chemical functionalization and viscosity, the molding process of soybean resins is similar to that of conventional thermosetting liquid molding resins, using resin transfer molding (RTM), vacuum-assisted resin transfer molding (VARTM), sheet molding compound (SMC), etc. The triglyceride-based materials display the necessary rigidity and strength required for structural applications. Also, some, but not all, soybean resins can be made to be biodegradable.[11]

The U.S. poultry industry generates more than one billion kilograms of feathers annually as a byprod-

Correspondence to: R. P. Wool (wool@ccm.udel.edu).
Contract grant sponsor: Environmental Protection Agency.
Contract grant sponsor: Department of Energy.

uct.[12] Disposal of the feather waste is expensive and difficult. For example, poultry waste is burned, buried, or recycled into animal feed and these methods are environmentally unsound and restricted. A more expensive disposal method is the production of a low-quality protein animal feed for which the demand is low. Some efforts have been made to develop processes for making fiber materials from feather wastes.[8,9] Feathers are made from the protein keratin and there are two forms of microcrystalline keratin in feathers: the fiber and the quill. The thermal energy required to perturb the molecular order of the quill is lower than that required for the fiber.[13] Thus, the feather fibers, with α-helical structure at the molecular level, are light and tough enough to withstand both mechanical and thermal stress. Due to the inherent danger of flying, natural selectivity has produced feather material of a very high quality. With the hollow structure of the keratin fibers, a given volume of the fiber innately contains a significant volume of air, presenting low-density ($SG \approx 0.80$) and low-dielectric constant ($k \approx 1.7$) suitable for composite and electronic materials.[14] The use of the avian feathers in composites as reinforcing fibers, after removal of the large quill, offers an environmentally benign solution for feather disposal and also presents to poultry producers a new route to reduce waste disposal costs and to gain a profit from feather waste.

The overall objective of this study is to develop a new composite from soybean (S) oil and KF and to conduct a fundamental study of the KFS material properties. The development of low-k dielectric materials is considered to be one of the main issues in modern high-speed microelectronics. The physical performance, such as strength, stiffness, vibration damping, and density, are important properties in automotive, trucking, farming equipment, civil infrastructure, defense, aerospace, civil infrastructure, housing construction, and electronic materials applications. The new soybean oil–keratin fiber (KFS) composite presented herein is an affordable, bio-based, and environmentally friendly material.

EXPERIMENTAL

Sample preparation

Acrylated epoxidized soybean oil (AESO, Ebecryl 860, UCB Chemical Co., Atlanta, GA) and soybean oil pentaerythritol glyceride maleates (SOPERMA)[15] were used with 33 wt % of styrene comonomer (Aldrich) as liquid molding resins, as described elsewhere.[1] The AESO contained three to four acrylate groups per triglyceride. The SOPERMA contained mole ratios of 1 : 3 : 7.6 of soy oil, pentaerythritol, and maleic anhydride, respectively. KF from chicken feathers and their fiber mats were obtained from Tyson Foods, Inc. Nonwoven keratin fiber mats were prepared in two different ways. One KF mat was made by adding 3 wt % of binder, and another (hybrid mat) was a KF–glass hybrid with 15 wt % of glass fiber. Composites were prepared with $\approx$ 0, 5, 10, and 20 wt % of the KF, which were mixed physically with the resin prior to molding. Because of the large volume occupied by the KF and related process difficulties, 20 wt % of the fibers was found to be a practical limit for physical mixing under ambient conditions. Therefore, the 30 and 45 wt % KF composites were prepared by using a VARTM process with the KF mats, where the resin was infused into the dry KF mats in a mold, using a vacuum.

The free-radical reactions of soy oil resin were carried out at elevated temperatures, and at room temperature by using different imitators. For high-temperature (HT) curing, tert-butyl peroxybenzoate (Aldrich) was added as an initiator. Initiator (1.5 wt %) was added for the AESO resin and 2.0 wt % was added for SOPERMA. High-temperature curing of the KFS composites was done at 90°C for 3 h and at 120°C for 3.5 h for the SOPERMA resin. Postcuring was done at 120°C for 2 h for the AESO resin, and at 150°C for 1 h for the SOPERMA resin. For room-temperature (RT) curing, cumyl hydroperoxide (Trigonox 239A, Akzo Chemicals) and methyl ethyl ketone peroxides (MEK, Witco) were used as an initiator, and cobalt naphthenate with 6% metal content (CoNap, Witco) was used as an accelerator. After room temperature curing for 24 h, the RT-cured AESO samples were postcured at 120°C for 2 h, and SOPERMA was postcured at 150°C for 1 h. After the total cure cycle was complete, the samples were cut and polished for various tests.

Characterization

The storage modulus and glass transition temperature (T_g) of the KFS composites were measured by using a dynamic mechanical analyzer (DMA 2988, TA Instruments) at a heating rate of 5°C/min according to ASTM D5023. The T_g was obtained from the maximum value of Tan δ.

A fast Fourier transform (FFT) analyzer (OROS PC Pack) was used to measure the vibration-damping properties[16] of AESO resin with different concentrations of comonomer. The sample dimensions were 6 $\times$ 190 $\times$ 250 mm. The sample was placed on two parallel rubber cords at room temperature. A moving hammer with a force transducer was used as the impulse exciter. The data were obtained from the accelerometer placed at both ends of the sample and the instrumented hammer. The data were averaged three times in the frequency domain to reduce noise. Postprocessing software (MEscopeVES) was used to obtain the results.

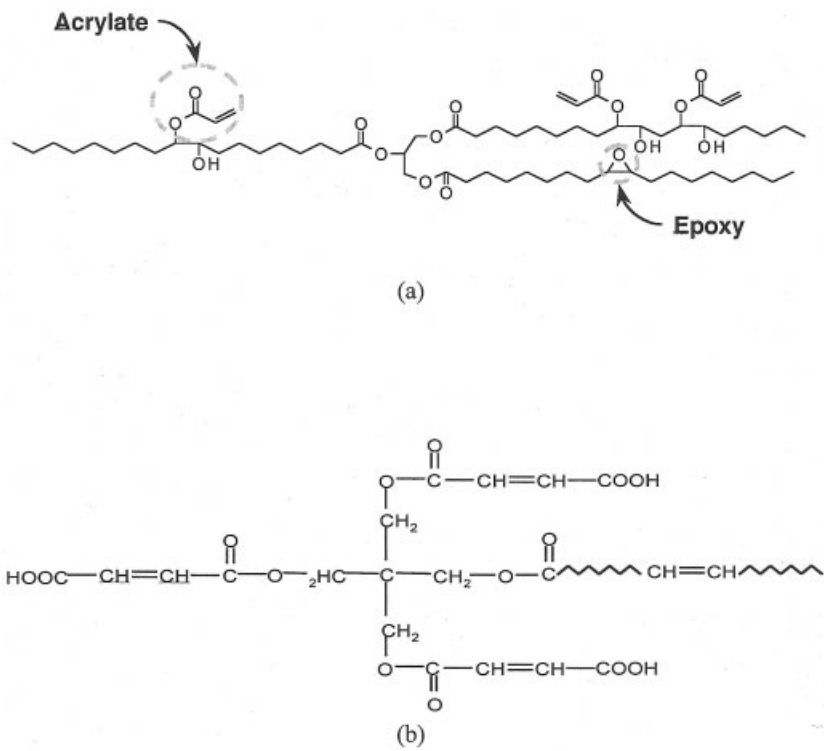

Figure 1 The molecular structure of (a) a typical acrylated epoxidized soybean oil (AESO)[1] and (b) soybean oil pentaerythritol glyceride maleates (SO : PER : MA).[15]

The dielectric properties of the materials were measured on dielectric analyzer (DEA 2970, TA Instruments) with a heating rate of 2°C/min at a frequency of 100 Hz. The dimension of a sample was 0.7 × 25.4 × 25.4 mm. In the dielectric analysis, each sample was placed between two gold electrodes (parallel plate sensors, TA Instruments).

The coefficients of thermal expansion (CTE), in-plane direction, were measured by using a thermomechanical analyzer (TMA 2940, TA Instruments) under a force of 0.05*N* at a heating rate of 5°C/min.

Water absorption tests of the composites were performed at room temperature in accordance with ASTM D570. The dimensions of the test specimens were 0.7 × 25.4 × 25.4 mm. The samples were placed in vials of distilled water and their weight change was determined with time.

The fracture toughness K_{1c} and the fracture energy G_{1c} of the composites were performed according to ASTM D5045-99 (three-point bending) at room temperature. The dimensions of the sample were 6.35 × 12.70 × 63.5 mm. The crosshead speed of the tensile tester (Instron 4201) was 1.27 mm/min (0.05 in./min).

The fracture surfaces of the composites were examined by scanning electron microscopy (SEM, JEOL JXA-840). The fracture surfaces were coated with gold by using a sputter coater (Denton Vacuum Inc.).

The flexural tests were performed according to ASTM D790 at room temperature. The crosshead speed of the tester (Instron 4201) was 1.27 mm/min. The dimensions of the samples for the flexural test were 3.17 × 12.70 × 63.5 mm.

The tensile fracture strength of a KF fiber was measured by using an Instron tester (Mini 44). Adhesive tape was used to hold a couple of the fibers during the test. The crosshead speed was 1.27 mm/min. The diameter of the each fractured fiber was measured by using an optical microscope (Leitz, Metallux 3).

RESULTS AND DISCUSSION

Wetting and compatibility test

In this section, the compatibility between the AESO resin and KF fibers is investigated. A critical issue for composite fabrication and good property development is the ability of the resin to wet, or be compatible with, the fibers. The AESO resin was synthesized from the reaction of acrylic acid with epoxidized triglycerides to add chemical functionality, such as C═C double bonds and hydroxyls,[1] as shown in Figure 1(a). Keratin fibers have a typical diameter of 6 μm and length of 8 mm, with an aspect ratio of about 1000, as shown in Figure 2. The nodes and hooks on the hollow keratin fibers can improve the structural properties and increase the surface area in the composite. Chemically, the keratin fibers are composed of amino acids, the building blocks of protein. The amino acid se-

quences that cause the primary α-helical structure of feather keratin are similar among several avian species.[13] The preparation of the fiber mats from raw feathers includes the washing, sanitizing, and mechanical shredding/shearing. However, the original molecular properties of the fiber are preserved during these mat-forming procedures.[8,13]

Figure 3 shows the wetting test of both AESO resin and water on the KF mat. The AESO resin droplet spread out easily on the mat, whereas the water droplet did not during the 5-min time interval. The water droplet continued to remain for several hours until it evaporated. The AESO drop spread very rapidly, essentially doubling its wetted area in 10 s [Fig. 3(b)], before attaining its final wetted area, which is a competition between spreading and imbibition of the drop in the KF mats, as discussed in ref. [17]. The degree of resin spreading and imbibition in the mat depends on a number of parameters including the surface tension and rheology of the resin, and the surface chemistry and porosity of the mat. It is further known that for the long-time spreading in quasi-static regimes, adsorption kinetics and dynamic interfacial tensions are the factors that control wetting.[18] Note in Figure 3(c) the very small drop of water to the right of the larger water drop, which also has not wetted the keratin fibers. Therefore, keratin fibers are compatible with AESO resin and are hydrophobic. However, the SOPERMA resin has high viscosity and a hydrophilic structure because of a high acid number (237 mg KOH/g),[15] shown in Figure 1(b). A small drop of SOPERMA resin spread in the KF mat but the imbibition of the resin during a VARTM process did not take place because of less compatibility. Also, the KF contain a significant volume of air in the hollow microcrystalline structure. The wetting inside of the fiber is a critical issue for the low dielectric constant and the density of the composites. This issue will be discussed in the density section of this article.

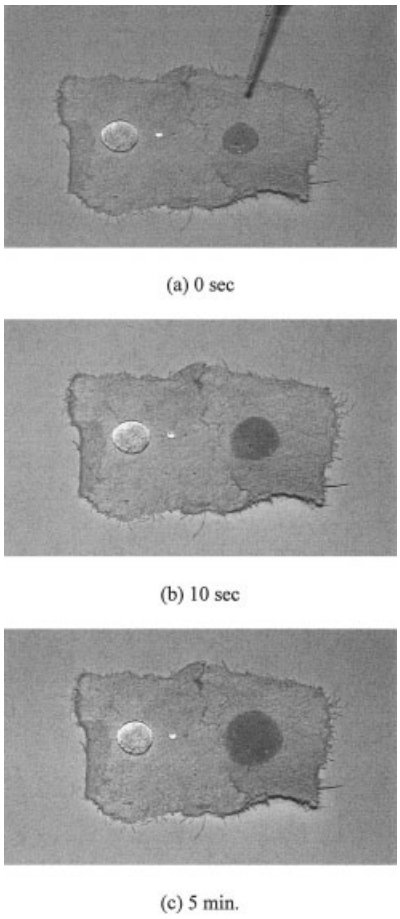

Figure 3 The wetting test of water (left) and AESO resin (right) on the KF mat.

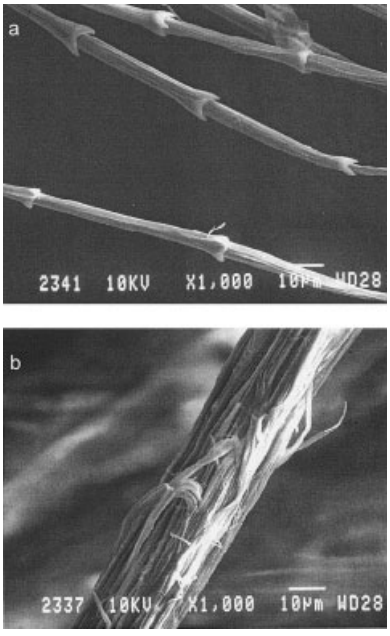

Figure 2 Scanning electron microscope (SEM) micrographs of feathers: (a) keratin fibers; (b) a small quill.

Effects of initiators and cure conditions

The objective of this experiment was to investigate the effects of chemical initiators and cure temperature on the properties of soybean oil based KF composites. The free-radical, chain-growth copolymerization reactions (or curing) in soybean oil based resin can be carried out either by thermal decomposition of the free-radical initiators at elevated temperatures or by redox decomposition of the free-radical initiators by using a metal promoter (accelerator) at low temperatures. For RT curing, the concentration of the initiators and an accelerator for the resins was varied to check the curability in 24 h. The results are shown in Table I for AESO and in Table II for SOPERMA, respectively. AESO was cured by cumyl hydroperoxides initiator

TABLE I
Curability Test of AESO Resin at Room Temperature

Cumyl peroxides	CoNap	
2.5%	0.3%	Partially cured
3.0%	0.8%	Cured
3.5%	0.8%	Cured
MEK peroxides	CoNap	
2.0%	0.5%	Not cured
2.0%	0.6%	Not cured
2.5%	0.6%	Not cured
3.0%	0.8%	Not cured
3.0%	1.0%	Not cured

with various amounts of accelerator, but was not cured by MEK peroxides. However, in the case of SOPERMA resin, it was cured by MEK peroxides, but was not cured by cumyl hydroperoxides. In low concentration of initiator and accelerator, a longer time is needed to complete the RT curing of the resins. As the extent of cure decreases, the T_g and modulus of the polymer decrease.[19]

The T_g and storage modulus of RT, and HT-cured AESO and SOPERMA resins at various concentrations of initiator and accelerator are given in Tables III and IV, respectively. Among the RT-cured polymers, the AESO properties were optimal at 3.0 wt % of cumyl hydroperoxide and 0.8 wt % of CoNap (after postcure), and those of SOPERMA at 3.0 wt % of MEK peroxides and 0.8 wt % of CoNap (after postcure). The T_g and storage modulus of the HT-cured polymer is higher than those of the RT-cured sample for both resins. This trend was also observed on the KFS composites. At HT, higher rates of reaction and higher conversions of double bonds in the soybean resin are expected. However, a HT reaction can have some process difficulties. It was hard to keep a vacuum during a HT VARTM process because of the evaporation of the styrene monomer. Also, the styrene vapor made voids or bubbles inside the composites during HT cure, leading to deterioration of mechanical properties. Generally, the selection of cure condition is motivated by processing and economic considerations. The low-temperature process can reduce the manufacturing cost. The focus of this study will be on the RT-cure reaction with 3.0 wt % of initiator and 0.8 wt % of accelerator for both resins.

TABLE III
T_g and Storage Modulus of RT and HT Cured AESO

Cure condition (Trigonox, % : CoNap, %)	T_g, °C	E' at 40°C, GPa
3.0 : 0.8, RT cured	66	1.247
3.0 : 0.8 (RT cured), after postcure	70	1.313
3.5 : 0.8, RT cured	64	1.095
3.5 : 0.8 (RT cured), after postcure	69	1.215
HT cured	79	1.642

Effects of the comonomer concentration

Soybean oil based resins can be blended with a comonomer such as styrene to improve its processibility and to control the composite properties to reach a range acceptable for structural applications. Styrene is used as a comonomer in commercial thermosetting resins and cures well with the soybean resins. By varying the amount of comonomer, it is possible to produce composite materials with different modulus, strength, and *Tg*.[20] Figure 4 shows the storage modulus of RT-cured AESO polymer at various styrene contents, as a function of temperature. The storage modulus at low temperature increased with increasing amount of styrene. In this rubbery region, the modulus is dominated by the copolymer effect of the higher modulus of polystyrene. However, at higher temperature (the plateau region), thermoset polymers behave according to rubber elasticity theory and the crosslink density, ν, is related to the modulus of elasticity, E,[21]

$$E = 3\nu RT \tag{1}$$

where R is the ideal gas constant, and T is the absolute temperature. The modulus determined from dynamic mechanical analysis is a measure of the effective crosslink density of polymers. Based on the fatty acid

TABLE II
Curability Test of SO : PER : MA Resin at Room Temperature

Cumyl peroxides	CoNap	
2.5%	0.3%	Not cured
3.0%	0.8%	Not cured
3.5%	0.8%	Not cured
MEK peroxides	CoNap	
2.0%	0.5%	Not cured
2.0%	0.6%	Partially cured
2.5%	0.6%	Partially cured
3.0%	0.8%	Cured
3.0%	1.0%	Cured

TABLE IV
T_g and Storage Modulus of RT and HT cured SO : PER : MA

Cure condition (MEKP, % : CoNap, %)	T_g, °C	E' at 40°C, GPa
2.0 : 0.6 (RT cured), after postcure	121	0.966
2.5 : 0.6 (RT cured), after postcure	122	1.019
3.0 : 0.8, RT cured	107	0.650
3.0 : 0.8 (RT cured), after postcure	128	1.039
3.0 : 1.0, RT cured	113	0.693
3.0 : 1.0 (RT cured), after postcure	129	1.027
HT cured	141	1.158

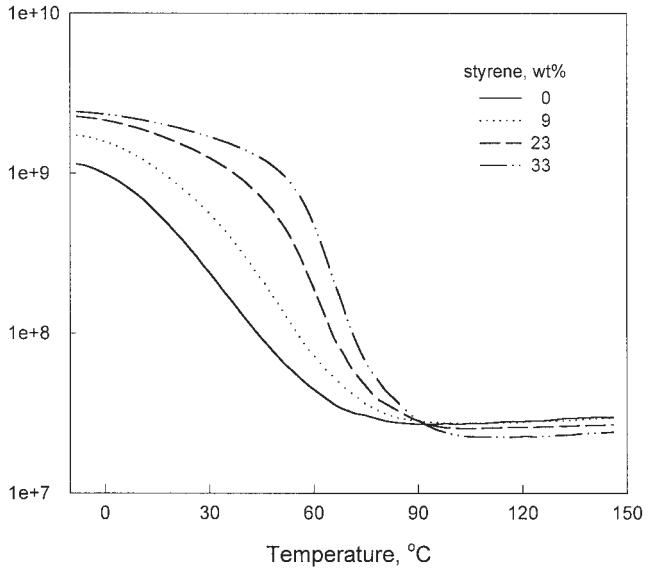

Figure 4 Storage modulus of RT-cured AESO at various styrene contents.

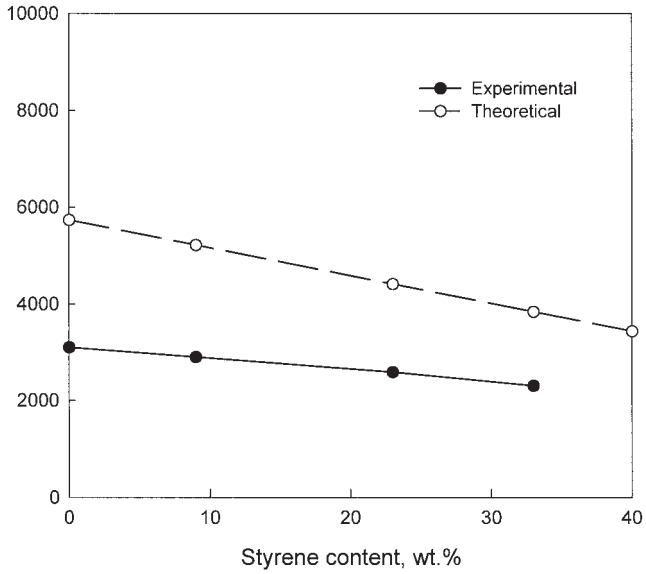

Figure 5 Comparison of experimental crosslink density of AESO resin with the theoretical values as a function of styrene content.

distribution of soybean oil, it is also possible to estimate the crosslinking ability of the triglycerides. The number of crosslinks in the network is a function of the composition of the resin and the functionality of the triglycerides. It is already known that AESO (Ebecryl 860) contains about 3.4 acrylates per triglycerides and the crosslinking functionality is 6.8 in the network for every triglyceride.[22] Therefore, if all of the acrylates on the triglycerides react, the crosslink density in the system is calculated[22] by

$$\nu = \frac{\text{MassFraction(AESO)} \times 6.8 \times \rho}{MW_{\text{AESO}}} \qquad (2)$$

where ρ is the density of the polymer and MW_{AESO} is the molecular weight of the AESO (1186 g/mol[22]). The calculated values are compared with experimentally determined crosslink densities in Figure 5. The crosslink density decreased linearly as the styrene mass fraction increased. As more styrene is present in the system, the crosslink density is lower because styrene is a linear chain extender and reduces the amount of crosslinking and thus, the modulus is lower in the plateau region of Figure 4. The theoretical crosslink densities are higher than the experimental values, which can be explained by intramolecular cyclization of triglycerides.[23] The intramolecular cyclization is the reaction of a functional group on a triglyceride with another functional group on the same triglycerides. The plasticization effect[22] by saturated fatty acids during the thermomechanical measurement can also be a reason for lower experimental crosslink densities.

In the case of random copolymers, or, miscible blends of polymers, the T_g of the copolymer or blend can be expressed by the Fox–Flory equation.[24]

$$\frac{1}{T_g} = \frac{w_1}{T_{g1}} + \frac{w_2}{T_{g2}} \qquad (3)$$

where w_1 and w_2 are the weight fraction of components 1 and 2 with T_{g1} and T_{g2}, respectively. The T_g of polystyrene is 373 K[25] and that of the pure triglycerides polymer is measured. Figure 6 shows the exper-

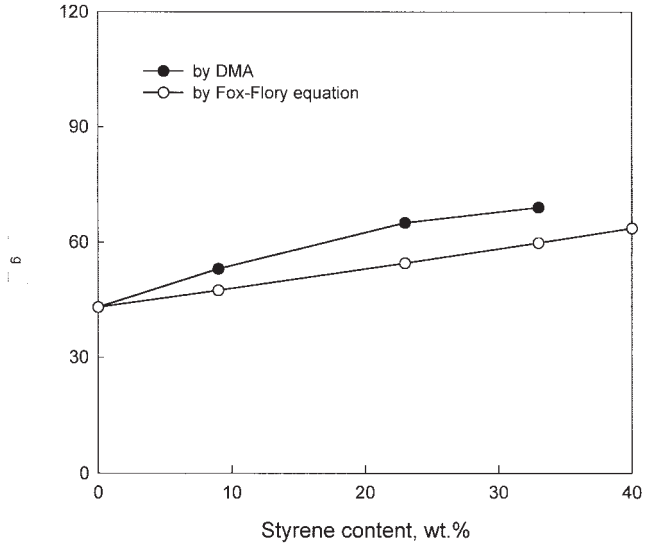

Figure 6 Glass transition temperature of RT-cured AESO as a function of styrene content.

imental T_g values measured by DMA and calculated values by using the Fox–Flory equation. The T_g was increased for the samples with an increase of styrene because the aromatic nature of styrene imparted rigidity to the network. Also, the samples had slightly higher T_g values than predicted. As comonomer was added, the efficiency of the polymerization increased, causing an increase of T_g. The crosslinking contribution can also be considered as a reason for the T_g increase.[20] The properties of these polymers can be controlled by different comonomers, degree of chemical functionality of the triglycerides, and extent of reaction during cure.[23]

Vibration-damping properties

Figure 7 represents the vibration-damping properties of RT-cured AESO resins at various concentrations of styrene comonomer and AESO-30 wt % KF composite, as a function of frequency. The passive damping materials and acoustic complex techniques are frequently used in various applications of automotive and aerospace structures to reduce vibrations and noise. As shown in Figure 7, the material damping, or its ability to dissipate vibrational energy, became lower with increasing styrene concentration in the resin. The triglycerides consist mostly of long aliphatic fatty acids that differ from the aromatic styrene monomer. The aromatic styrene monomer is much more restrictive to movement than the flexible aliphatic chains of the triglycerides. A larger number of relaxation modes are also available in triglycerides because of the broad fatty acid distribution.[22] As the amount of styrene in the copolymer increases, the chain mobility in the networks decreases, the modulus increases, and so the vibration damping decreases. The major damping mechanisms in vibration are due to the extensional and shear deformations of the structures viscoelastic material.[16]

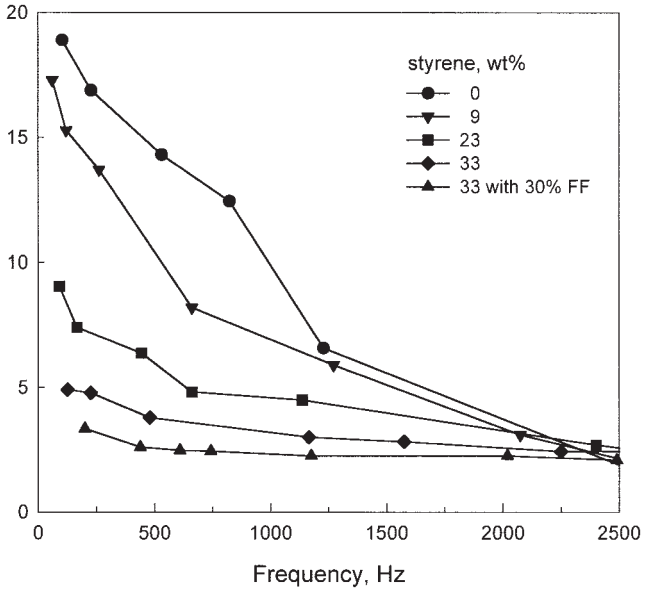

Figure 7 Vibration damping properties of RT-cured AESO at various amounts of styrene and AESO–30 wt % KF composite.

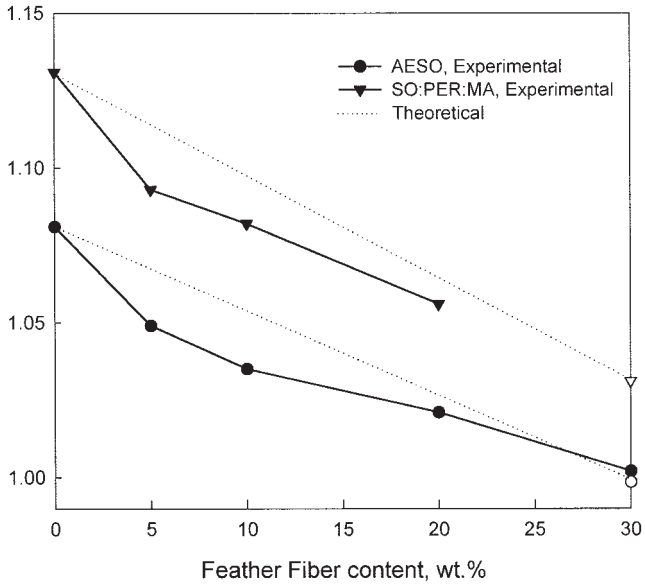

Figure 8 The density of RT-cured AESO and SO : PER : MA composites.

The damping property of AESO–30 wt% of KFS composite is also shown in Figure 7. The material damping is lowered with addition of keratin fibers. The increase in modulus (or stiffness) caused corresponding reduction of damping properties of the composite material. The increase in modulus of the KFS composites will be discussed in the thermomechanical property section.

Bulk density of the composites

Figure 8 shows the experimental and theoretical density of RT-cured AESO and SOPERMA composites as a function of the keratin fiber content. The theoretical density values are calculated by using the mixing rule,

$$\rho = w_1\rho_1 + w_2\rho_2 \quad (4)$$

where w_1 and w_2 are the weight fraction of components 1 and 2 with ρ_1 and ρ_2, respectively. The density of the hollow keratin fiber is 0.80 g/cm^3, and those of AESO and SOPERMA resins are 1.08 and 1.13 g/cm^3, respectively. The density of the composites decreased (Fig. 8) with an increase of the keratin fiber concentration for both resins. This contrasts with a density of typical composites from synthetic reinforcing fibers. The keratin fibers are hollow and light materials and contain air in the hollow structure. Lightweight mate-

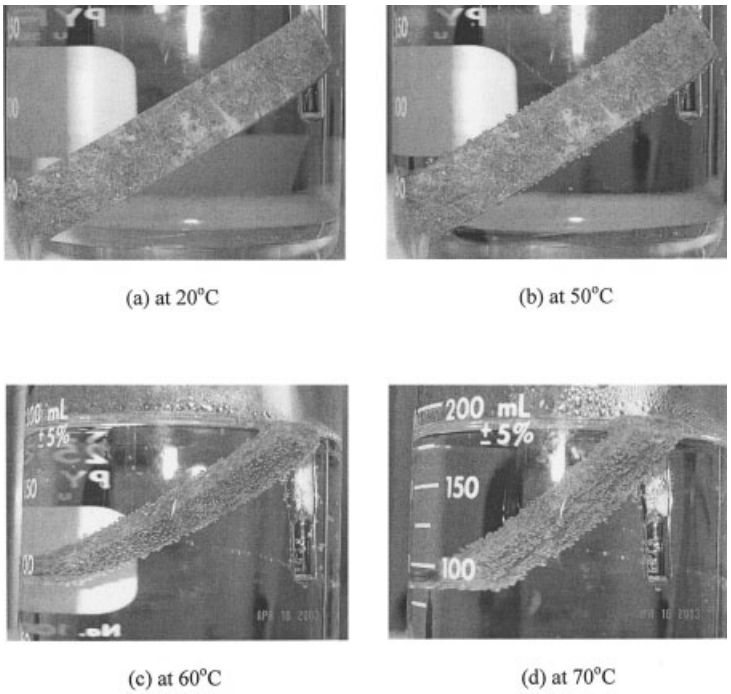

Figure 9 AESO-30 wt % KF composites in water at a heating rate of 1°C/min.

rials make a significant impact on fuel consumption for automotive and trucking applications. Also, the density of the composite can be made to be less than 1 g/cm^3 at about 30 wt % of keratin fibers for AESO resin and at about 40% for SOPERMA. As shown in Figure 8, the experimentally measured values are lower than the theoretical density for physically mixed samples (5, 10, and 20 wt %), but the measured density is slightly higher for a VARTM processed sample. During physical mixing, trapped and entrained air between the keratin fibers remains in the composite, resulting in a lower density than expected. However, in the case of the VARTM sample, a vacuum process sucks out the air between the fibers and some of hollow fibers are filled by resin infusion. The experimental density for the AESO–30 wt % KFS composite (prepared by VARTM process) was 1.001 g/cm^3, which is the theoretical value for the 28.4 wt % KF composite. This means that about 5% filling of the hollow keratin fibers occurred during the VARTM process, but the rest of the fibers (95%) in the composite still contained a significant volume of air.

The AESO–30 wt % KFS composite was heated in water to check if there was air inside the composite and to explore the unique possibility of convective cooling, as shown in Figure 9. One can see lots of air bubbles on the surface of the composite at elevated temperatures and the number of air bubbles from the composite increased with increasing temperature. The blank (AESO, no KF) sample did not show similar behavior, which could have been explained by simple bubble nucleation phenomena on the surface of the resin. The convective cooling due to the flow of air from the hollow feathers could be determined from the mass flow rate of air, the heat capacity of air (42 J/mol °C), and the temperature change. The low-density, high-air content of the KFS composites makes them suited to electronic applications, as well as automotive and aeronautical applications.

Dielectric properties of the composites

In a typical microchip, performance gain is mostly limited by the intra- and interlayer capacitance, dictated primarily by the dielectric constant (k) of the insulators, known as dielectrics.[26] A decrease of the k value of the insulator containing the printed circuits increases the operating speed, minimizes the cross-talk effects between metal interconnects, and diminishes the power consumption.[27] The delay time of the electronic signal is proportional to the square root of k and values close to $k = 1$ are most desirable. Figure 10 shows the k values of the KFS composites developed from hollow keratin fibers and AESO resin, at a temperature of 25°C. The k values decrease linearly from 2.7 to 1.7, with an increase of the keratin fiber content approximately as

$$k_{KFS} = k_{AESO}(1 - w_{KF}) + k_{KF}w_{KF} \quad (5)$$

where w_{KF} is the weight fraction of hollow keratin fibers. The KFS composite has a lower dielectric con-

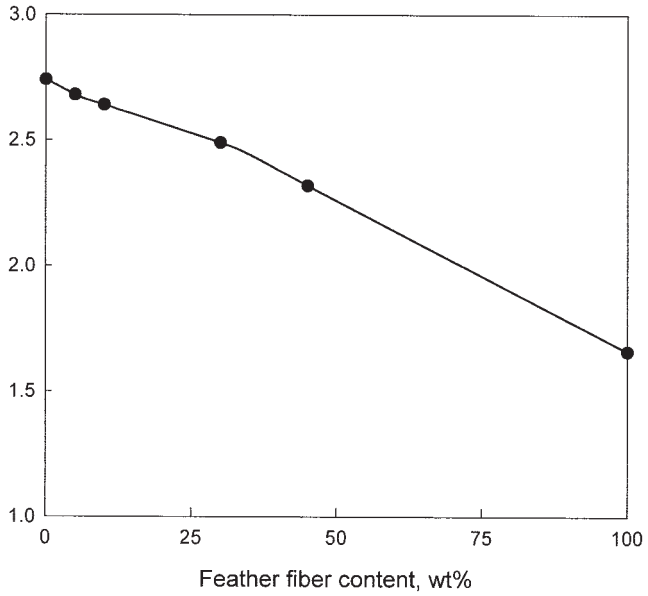

Figure 10 The dielectric constants of AESO composites at a temperature of 25°C.

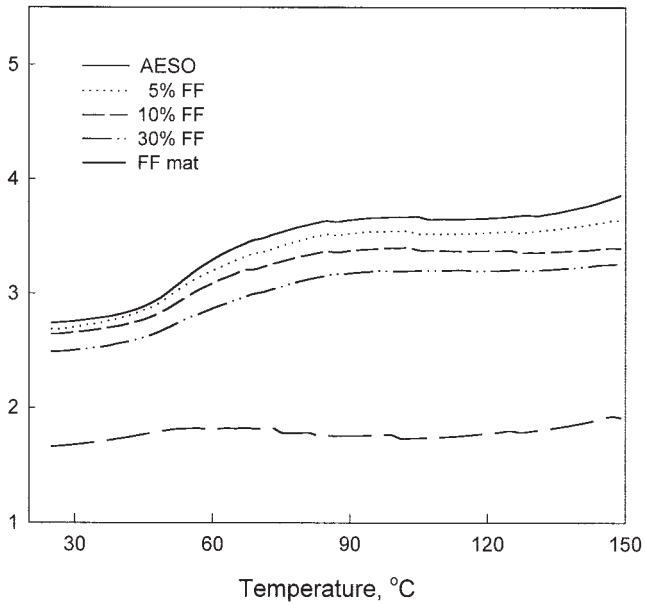

Figure 11 The temperature dependence of the dielectric constants of AESO composites.

stant than conventional semiconductor insulators such as silicon dioxide (k = 3.8–4.2[27]), epoxies, polyimides, and other dielectric materials. The measured k_{KF} value of the KF mat itself was 1.7 because hollow keratin fibers contain a significant volume of air. The ideal minimum k value is 1.0, as represented by air and therefore, a porous or high-air content material may have dielectric constants in the ultralow-k (<2.2) region.[26] The low-cost KFS composite has the potential to replace the dielectrics in microchips and circuit boards in the ever-growing electronic materials field, in addition to many applications as a new light-weight composite material. Thermosetting epoxy resin has a k value of 4.1 and is used for electromagnetic component (EMC), printed circuit board (PCB), and the resin-encapsulating-type semiconductor devices.[28] The k value of AESO resin itself is 2.7 and the molding process of soybean resin can follow the lead of conventional unsaturated polyester or vinyl ester resins. The low-viscosity resins are also capable of being spun into nanosize thin films. Thus, a low-polarity soybean resin alone can also be a substitute for petroleum-based resins in many electronic material applications.

The temperature dependence of the dielectric constant of the AESO-KF composites is shown in Figure 11. The dielectric constant of the KFS composite slightly increased with increasing temperature, resulting from the alignment of the dipoles when the composite softened with temperature. However, because the effect of temperature on the k value of air is minimal, we expect relatively little change as noted for the pure KF mat (lower curve) in Figure 11.

Thermal expansion of the composites

The CTE of the AESO–KF composites are shown in Table V. The CTE is defined as the fractional change in length divided by the change in temperature

$$\alpha = \frac{K}{L_0}\left(\frac{\Delta L}{\Delta T}\right) \tag{6}$$

where α is the CTE (μm/m°C), L_0 is the initial sample length (m), ΔL is the change in sample length (μm), ΔT is the change in temperature, and K is the cell constant (normally 1.000). From an atomic perspective, the CTE reflects an increase in the average distance between atoms with increasing temperature.[29] The change in bond length is due to the anharmonicity of the bonding, and generally, weaker bonds have a higher CTE value. The CTE of the KFS composites decreases with increasing keratin fiber content and these values are quite low, especially for the 30 wt % sample. The 30 wt % KF sample is a VARTM sample using the KF mats and the fibers are highly oriented in the in-plane di-

TABLE V
The CTE Values of AESO–KF Composites

KF content, wt %	α below T_g, μm/m°C	α above T_g, μm/m°C
0	127.2	205.8
5	106.1	200.6
10	100.4	196.3
20	93.1	193.2
30	67.4	69.6

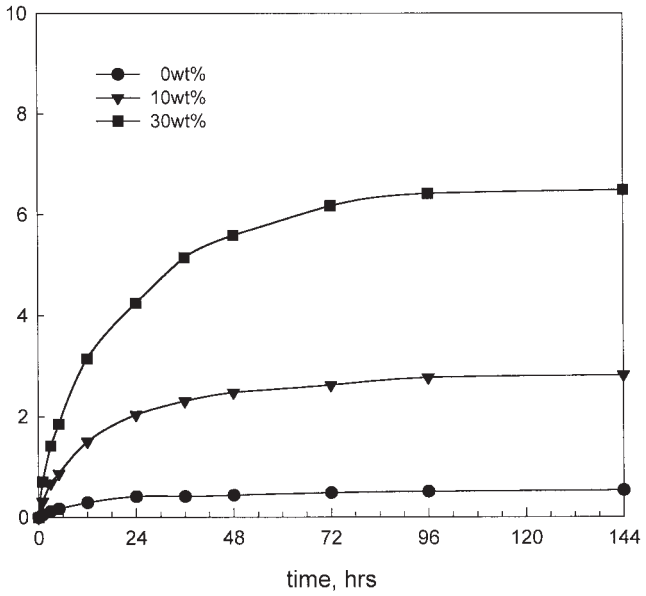

Figure 12 The water absorption of RT-cured AESO–KF composites.

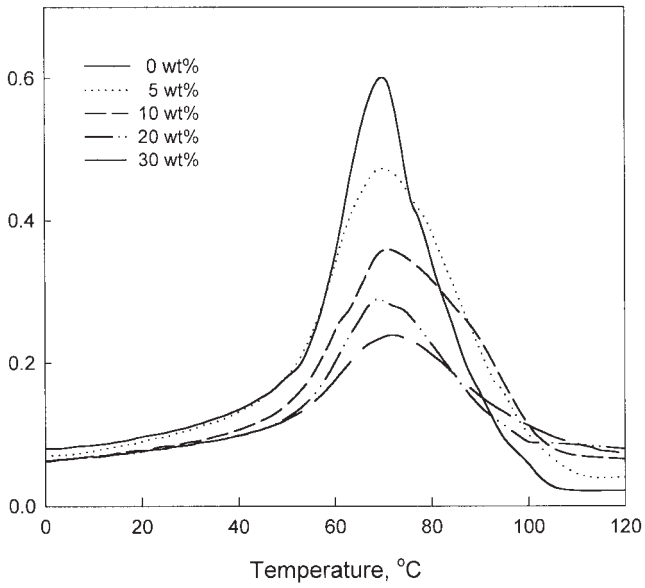

Figure 14 Tan δ of RT-cured AESO–KF composites.

rection. The CTE, below the T_g, of the 30 wt % composite is 67.4 μm/m°C (or ppm/°C). The value is low enough for electronic applications and similar to the value of silicon material (66 ppm/°C)[30] or polyimides (≈59 ppm/°C).[31] However, the CTE of the AESO is higher and changes abruptly above its T_g. The thermal expansion of AESO resin is compensated with the thermal contraction of keratin fibers in the longitudinal (oriented) direction. Interactions between resin and keratin fibers also act to resist changes in dimension with increasing temperature. The CTE can be further decreased by increasing the T_g and crosslinking density of the network structure, resulting in increasing chain stiffness. The AESO resin molecular structure used in these examples was not optimized in accord with the rules for property optimization suggested by LaScala and Wool,[23] and much room for improvement exists.

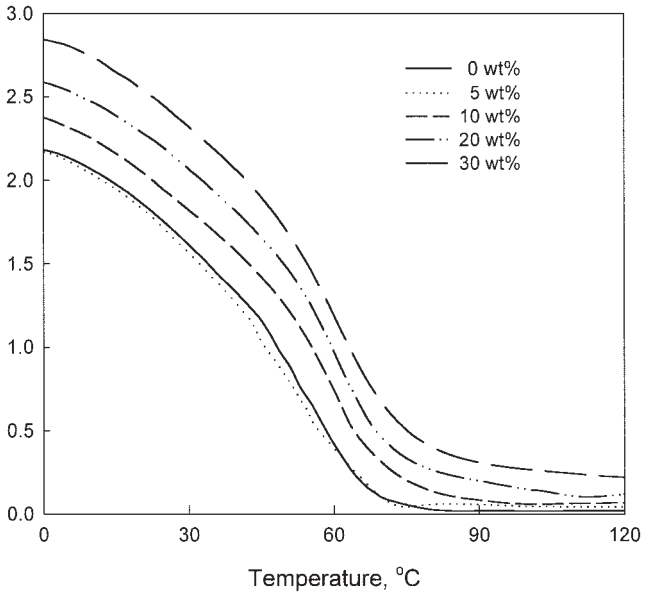

Figure 13 Storage modulus of RT-cured AESO–KF composites.

Water absorption of the KFS composites

The water absorption of RT-cured AESO KFS composite is shown in Figure 12, as a function of time. At equilibrium (after 6 days), the AESO polymer (0 wt % of KF) increased in weight by 0.5%, while the 30 wt % KF composite increased by 6%. The AESO resin and keratin fibers have hydrophobic properties. However, the exposed hollow keratin fibers soaked up water by capillary action and the feathers have both hydrophobic and hydrophilic properties at the molecular level.[13] The measured water uptake is dependent on the keratin fiber content and the dependence of the initial slope of the sorption curves indicates a significant

TABLE VI
Storage Modulus (E') and T_g of RT-Cured AESO Composites

KF content, wt %	E' at 40°C, GPa	T_g, °C
0	1.313	70
5	1.291	70
10	1.598 (+21.7%)	71
20	1.836 (+39.8%)	70
30 (KF mat)	2.085 (+58.8%)	71

TABLE VII
Storage Modulus (E') and T_g of RT-Cured SO : PER : MA Composites

KF content, wt %	E' at 40°C, GPa	T_g, °C
0	1.039	128
5	1.082 (+4.1%)	129
10	1.139 (+9.6%)	128
20	1.072 (+3.2%)	127

dependence of the diffusion coefficient, D, on the fiber concentration. The kinetic study of the sorption in polymers as a means of determining the diffusion coefficient has widely been used. In general, the partial differential equation for mass transfer (diffusion) is expressed as

$$\frac{\partial C}{\partial t} = D\left(\frac{\partial^2 C}{\partial x^2}\right) \tag{7}$$

where C is the concentration at time t, and distance x, from the polymer surface. For an infinite slab with a constant D and at short times,[32]

$$\frac{M_t}{M_\infty} = \frac{4}{L}\left[\frac{Dt}{\pi}\right]^{1/2} \tag{8}$$

where M_t is the amount of water sorption at time t, M_∞ is the equilibrium sorption, and L is the thickness of the sample. The initial slope method from Fick's second law is commonly used to determine the diffusion coefficient (D) from the initial gradient of a graph of M_t/M_∞ as a function of t. The diffusion coefficient for the pure AESO resin is $D = 4.43 \times 10^{-9}$ cm^2/s; for 10% KFS composite, $D = 5.28 \times 10^{-9}$ cm^2/s; and for 30% KFS composite, $D = 5.48 \times 10^{-9}$ cm^2/s. The AESO resin reached equilibrium in 36 h, whereas the 30% KF-composite required 96 h. The measured water diffusion coefficient in the composites is dependent on the keratin fiber content and sorption through the fiber is dominant. In comparison with other natural fibers, the water uptake of the AESO–30 wt % KFS composite (6%) is less than that of the AESO–30 wt % flax composites, which has a 12.4% increase at equilibrium.[2]

Thermomechanical properties of the composites

Dynamic mechanical measurements over a wide temperature range are useful in the understanding of the viscoelastic behavior and provide valuable insights into the relationship between structure and properties of composite materials. Figure 13 shows the storage modulus E' of RT-cured AESO KFS composites as a function of temperature at various concentrations of keratin fibers. The storage modulus was significantly improved with the addition of keratin fibers over the whole range of the testing temperature. A change in the modulus indicates a change in rigidity and, hence, strength of the composite.

Tan δ, the ratio of viscous to elastic properties, of RT-cured AESO–KFS composites versus temperature is shown in Figure 14. The maximum value of Tan δ decreases with an increase of the fiber content, indicating the increasing trend of composite rigidity. The lowering of Tan δ values, the damping energy ratio, suggests the restraint effect of the fibers on the matrix mobility,[33] and this restriction is enhanced with an increasing fiber content. This is the reason the vibration damping was lowered with addition of keratin fibers, as shown in Figure 7. Also, the damping peak becomes broader with increasing fiber content because of many kinds of relaxation modes of polymer chains due to the reinforcing fibers.

The storage modulus and T_g of the RT-cured AESO composites are tabulated in Table VI. The storage modulus of the 30 wt % KFS composite improved 58.8% in comparison with the pure AESO polymer. This is important for electronic materials, because the desired addition of air to obtain low-k materials typically results in reduced strength and stiffness. The T_g was not significantly influenced by the addition of keratin fibers. Table VII shows the storage modulus and T_g of RT-cured SOPERMA composites. The properties showed the same trend as the AESO composites. However, the enhancement of the modulus is much lower than that of AESO composites.

Mechanical properties of the composites

The addition of keratin fibers improves the mechanical properties of the KFS composites. The fracture prop-

TABLE VIII
Fracture Properties of RT-Cured AESO Composites

KF content, wt %	Max. load N	Fracture toughness K_{ic}, MPa m$^{1/2}$	Fracture energy G_{ic}, KJ/m^2
0	97.6	1.458	1.420
5	97.1	1.455 (−0.2%)	1.610 (+13.4%)
10	103.0	1.524 (+4.5%)	1.759 (+23.9%)
20	113.0	1.672 (+14.7%)	1.820 (+28.2%)
30 (KF mat)	120.1	1.768 (+21.3%)	1.927 (+35.7%)
30 (hybrid mat)	130.7	1.931 (+32.4%)	1.945 (+37.0%)

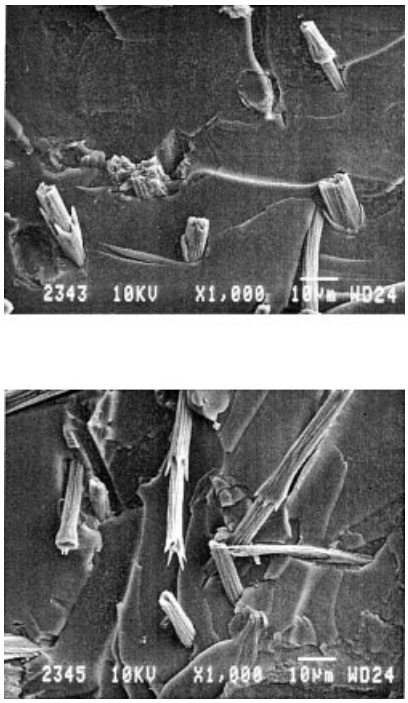

Figure 15 SEM micrographs of the fracture surface of 5 wt % AESO–KF composites.

erties of RT-cured AESO composites are shown in Table VIII. The fracture toughness (K_{ic}) and the fracture energy (G_{ic}) increased with an increase of keratin fiber content. The K_{ic} of AESO resin increased 21.3% and the G_{ic} improved 35.7% by adding 30 wt % KF. This result is gratifying because the introduction of such natural fibers with high air content and potential defects could have resulted in a considerably weaker material. The improvement in properties also attests to the evolution of high-performance fibers required for long duration flight by the avian species. The composites prepared by using hybrid mats also showed better properties than pure KF mats composite. The hybrid mat is a mixture of 15 wt % of glass fibers with keratin fibers. Glass fibers are the most widely used synthetic fibers for general reinforcement of polymers. The high stiffness and strength (1.5 GPa) of glass fibers gave the composite higher toughness properties.

The SEM micrographs of the fracture surfaces of RT-cured AESO composite with 5 wt % keratin fibers are shown in Figure 15. The keratin fibers were broken without complete pullout during the fracture process. It indicates that adhesion between AESO resin and keratin fibers is quite good for reinforcing. The nodes and hooks on the feather fibers increase the wetted surface area and improve the structural properties of the composite. The mechanical properties of composites depend on the properties of the matrix and the fiber, and the bond strength, among other factors.

The fracture energy G_{ic} of a keratin fiber can be evaluated by using the nail solution.[34] The composites

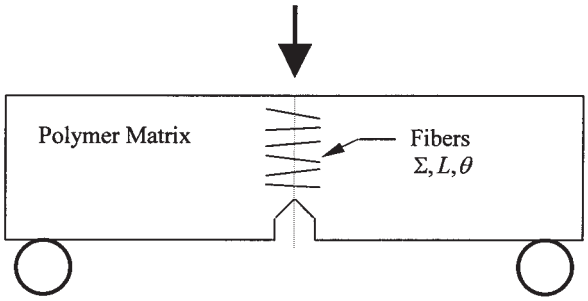

Figure 16 Schematic of the composite nailed by Σ number of the keratin fibers.

are nailed together by Σ fibers per unit area, of length L, shown schematically in Figure 16. The fracture strength of the fibers is obtained[34] as

$$G_{IC}(f) = \frac{1}{2}\mu_0 \Sigma L^2 V^{\alpha} \tag{9}$$

where μ_0 is the unit length friction coefficient and V is the pullout velocity. For static friction control of the pullout process ($\alpha = 0$),

$$G_{IC}(f) = \left(\frac{1}{2}\mu_0 L\right) L\Sigma \tag{10}$$

Here, $(1/2\mu_0 L)$ is the force to pullout a single fiber and L is the distance. Therefore, the total energy for fibers in the composite is represented as

$$G_{IC}(f) = G_1 \Sigma \tag{11}$$

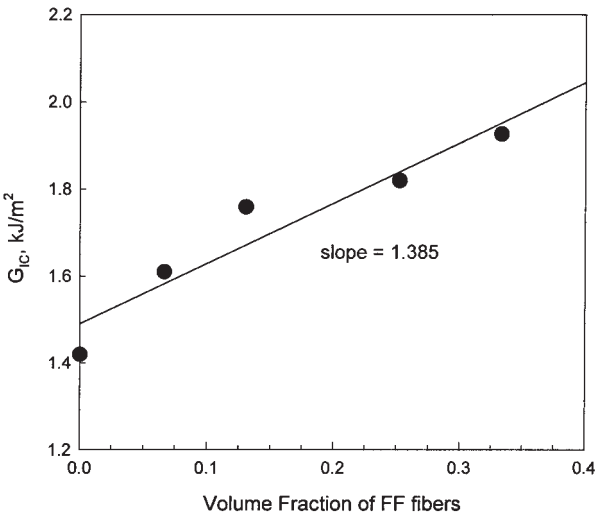

Figure 17 The fracture energy of RT-cured AESO composites as a function of volume fraction of keratin fibers.

TABLE IX
Fracture Properties of HT-Cured AESO Composites

KF content, wt %	Max. load N	Fracture toughness K_{ic}, MPa $m^{1/2}$	Fracture energy G_{ic}, KJ/m^2
0	114.3	1.725	1.510
5	121.0	1.800 (+4.3%)	1.965 (+30.1%)
10	126.4	1.872 (+8.5%)	1.979 (+31.1%)
20	126.6	1.873 (+8.6%)	1.677 (+11.1%)

It was assumed that there is not complete pullout of fibers because they fracture at some critical length. Here, G_1 is the energy to break one fiber,

$$G_1 = G_f^0 a_f \tag{12}$$

where G_f^0 is the fracture energy of the composite when the fiber volume fraction is 1 and a_f is the area of a fiber with a diameter, d, represented as

$$a_f = \frac{\pi d^2}{4}\beta \tag{13}$$

where, β is a geometric factor [$=1(\cos^2\theta)$], θ is the angle of fiber orientation, and Σ can be represented as the volume fraction of the fibers (ψ)

$$\Sigma = \phi h = \frac{\psi}{\nu_1} h = \frac{4\psi\cos^2\theta}{\pi d^2} \tag{14}$$

where ϕ is the number of the fibers per unit volume, $h = L\cos^2\theta$, and ν_1 is the volume of a fiber. Therefore, the total energy for fibers is

$$G_{IC}(f) = G_1\Sigma = \psi G_f^0 \tag{15}$$

The total energy for composites (polymer matrix and fibers) is

$$G_{total} = G_{IC}(M) + G_{IC}(f) \tag{16}$$

and

$$G_{IC} = (1 - \psi)G_M^0 + \psi G_f^0 = G_M^0 + (G_f^0 - G_M^0)\psi \tag{17}$$

The fracture energy of AESO composites is plotted in Figure 17 as a function of volume fraction of keratin fibers. The intercept is the fracture energy of the polymer matrix ($G_M{}^0$) and the slope represents ($G_f{}^0 - G_M{}^0$). From Figure 17, $G_f{}^0 = 2.80\ 5$ kJ/m^2. The fracture stress ($\sigma_f = G_f{}^0/\delta$) of keratin fiber can be calculated as σ_f = 93.5–187.0 MPa ($\delta = L_{Max}$ = 30–15 μm). The experimentally measured tensile fracture strength of keratin fiber was in the range of 41.4–129.7 MPa due to the heterogeneity of the fibers.

Table IX shows the toughness properties of HT-cured AESO composites. The properties were improved by adding keratin fibers and the HT-cured AESO polymer (0 wt %) has a higher toughness property than RT-cured resin. However, the voids and cracks, due to the evaporation of styrene at high temperature, leads to deterioration and fluctuation of the composite properties. Table X gives fracture properties of the RT-cured SOPERMA composites with various concentrations of keratin fibers. The fracture toughness and the energy are greatly enhanced with an increase of the fiber content, despite lower compatibility. The toughness properties of SOPERMA resin itself are much lower than those of AESO resin. Therefore, the reinforcing effect of keratin fibers is greater on SOPERMA composites.

Table XI shows the flexural yield strength and flexural modulus of the RT-cured AESO composites. The flexural properties were significantly enhanced with the addition of keratin fibers. The sample prepared by using hybrid mats (15% glass fibers) shows much higher flexural properties, due to the high stiffness of glass fibers. Therefore, the keratin fiber, itself or hybrid, is a possible substitute for synthetic

TABLE X
Fracture Properties of RT-Cured SO : PER : MA Composites

KF content, wt %	Max. load N	Fracture toughness K_{ic}, MPa $m^{1/2}$	Fracture energy G_{ic}, J/m^2
0	26.9	0.402	63
5	32.9	0.507 (+18.6%)	148 (+134.9%)
10	45.4	0.688 (+66.7%)	340 (+439.7%)
20	51.3	0.778 (+88.2%)	515 (+717.5%)

TABLE XI
Flexural Properties of RT-Cured AESO Composites

KF content, wt %	Flexural yield strength, MPa	Flexural modulus of elasticity, GPa
0	34.807	0.896
5	36.178 (+3.9%)	0.971 (+8.4%)
10	36.762 (+5.6%)	1.288 (+43.8%)
20	38.782 (+11.4%)	1.489 (+66.2%)
30 (CF mat)	45.225 (+29.9%)	1.588 (+77.2%)
30 (hybrid mat)	57.791 (+66.0%)	1.938 (+116.3%)

fibers used for reinforcement of composite materials.

CONCLUSION

In this study, the affordable, bio-based, and environmentally friendly composite materials from soybean resins and hollow keratin fibers were developed and their fundamental properties were investigated.

Keratin fibers are hollow, light, hydrophobic, and compatible with AESO resin. The modulus of AESO resin in the rubbery region and T_g were increased with increasing styrene comonomer content. However, The crosslink density decreased linearly with an increase of styrene content.

The density of the composites decreased with increasing keratin fiber content and can be made to be less than 1 g/cm^3. About 5% of hollow keratin fibers were filled by resin infusion during the VARTM process, but the composite still contained a significant volume of air in the hollow structure of the fibers. The k value of the AESO–KFS composite was found to be in the range of 1.7–2.7, depending on the hollow fiber fraction. The k values were lower than that of a conventional semiconductor insulator material such as silicon dioxide, epoxies, polyimides, and other dielectric materials. The coefficient of thermal expansion of the new composite material (67.4 ppm/°C) was low enough for electronic applications, and similar to the value of silicon material or polyimides. The measured water absorption of AESO resin was 0.5% and the diffusion coefficients of AESO-KFS composites are dependent on keratin fiber content and sorption through the fiber is dominant. The storage modulus of AESO composite was significantly improved with the addition of keratin fibers. The damping peak of the composite was lowered and the peak became broader with an increase of the fiber content. The fracture toughness and fracture energy of the composites were increased with increasing fiber content. The fracture energy of a keratin fiber in the composites was evaluated by using the nail solution. The mechanical properties of the new composite materials are in the acceptable range for composite applications.

New potential material uses for chicken feathers in the future include carbonization of chicken feathers by pyrolysis to make high-performance fibers.[35,36] We recently observed that the fibers retain their hollow structure and shrink affinely during pyrolysis but appear to have mechanical properties closer to graphite fibers. This could provide a new source of unusual light-weight, high-performance, low-cost fibers for composites, especially SMC. Also, in making new bio-based foams by high-pressure CO_2 reactions with functionalized triglycerides, it was observed that the chicken feather fiber acted as an excellent nucleating agent and stabilizer for the foam during the reaction.[37,38]

We thank Tyson Foods Inc. for providing keratin feather fibers. The authors gratefully acknowledge financial support from the Environmental Protection Agency and the Department of Energy.

REFERENCES

1. Khot, S.; LaScala, J.; Can, E.; Morye, S.; Williams, G.; Palmese, G.; Kusefoglu, S.; Wool, R. P. J Appl Polym Sci 2001, 82, 703.
2. Williams, G. I.; Wool, R. P. Appl Compos Mater 2000, 7, 421.
3. Can, E.; Kusefoglu, S.; Wool, R. P. J Appl Polym Sci 2001, 81, 69.
4. Thielemans, W.; Can, E.; Morye, S.; Wool, R. P. J Appl Polym Sci 2002, 83, 323.
5. Can, E.; Kusefoglu, S.; Wool, R. P. J Appl Polym Sci 2002, 83, 972.
6. LaScala, J.; Wool, R. P. J Am Oil Chem Soc 2002, 79 (1), 59.
7. LaScala, J.; Wool, R. P. J Am Oil Chem Soc 2002, 79 (4), 373.
8. Gassner, III, G.; Schmidt, W.; Line, M.; Thomas, C.; Waters, R. U.S. Pat. 5,705,030, 1998.
9. Gassner, G. U.S. Pat. 6,027,608, 2000.
10. Liu, K. Soybeans: Chemistry, Technology, and Utilization; Chapman & Hall; New York, 1997; pp. 25–95.
11. Mohanty, A. K.; Misra, M.; Hinrichsen, G. Macromol Mater Eng 1999, 276/277, 1.
12. McGovern, V. Environ Health Persp 2000, 108 (8), A366.
13. Schmidt, W. F. in Advanced Fibers, Plastics, Laminates and Composites; Wallenberger, F. T.; Weston, N. E.; Ford, R.; Wool, R. P.; Chawla, K. (Eds.); Materials Research Society, Warrendale, PA, 2002; pp. 25–32.
14. Wool, R. P.; Hong, C. K. U.S. Pat. (pending).
15. Wool, R. P.; Can, E. U.S. Pat. (pending).
16. Heylen, W.; Lammens, S.; Sas, P. Modal Analysis Theory and Testing; KU Leuven, Heverlee, Belgium, 1997.

17. von Bahr, M.; Kizling, J.; Zhmud, B.; Tiberg, F. in a Swedish National Program Paper Surfaces for Digital Printing (S2P2); Report S2P2 SS4.
18. von Bahr, M.; Tiberg, F.; Yaminsky, V. Colloids Surf A 2001, 193, 85.
19. Goodman, S. H. in Handbook of Thermoset Plastics; Goodman, S. H. (Ed.); Noyes Publications: Park Ridge, NJ, 1986; pp. 1–17.
20. Auad, M. L.; Aranguren, M.; Borrajo, J. J Appl Polym Sci 1997, 66, 1059.
21. Flory, P. J. Principles of Polymer Chemistry; Cornell Univ. Press: Ithaca, NY, 1975.
22. Khot, S. N. Synthesis and Application of Triglyceride Based Polymers; Dissertation, University of Delaware, NJ, Newark, 2001.
23. LaScala, J.; Wool, R. P. Polymer 2005, 46, 61.
24. Fox, T. G. Bull. Am Phys Soc 1956, 1, 123.
25. Brandrup, J.; Immergut, E.; Grulke, E. Eds., Polymer Handbook, 4th ed.; John Wiley & Sons, New York, 1999; p. VI 211.
26. Miller, R. D. Science 1999, 286, 421.
27. Treichel, H.; Withers, B.; Ruhl, G.; Ansmann, P.; Wurl, R.; Muller, Ch.; Dietlmeier, M.; Maier, G. in Handbook of Low and High Dielectric Constant Materials and Their Applications; Nalwa, H. S. (Ed.), Academic Press; San Diego, 1999; Vol. 1, Chapter 1.
28. Ogura, I. in Handbook of Low and High Dielectric Constant Materials and Their Applications; Nalwa, H. S. (Ed.); Academic Press; San Diego, 1999; Vol. 1, Chapter 5.
29. Callister, W. D. Material Science and Engineering: An Introduction, 3rd ed.; Wiley: New York, 1994.
30. Martin, S. J.; Godschalx, J. P.; Mills, M. E.; Shaffer II, E. O.; Townsend, P. Adv Mater 2000, 12, 1769.
31. Eichstadt, A. E.; Ward, T. C.; Bagwell, M. D.; Farr, I. V.; Dunson, D. L.; McGrath, J. E. J Polym Sci, Part B: Polym Phys 2002, 40, 1503.
32. Crank, J. The Mathematics of Diffusion, 2nd ed.; Oxford Univ. Press; Oxford, 1975.
33. Yu, S.; Hing, P.; J Appl Polym Sci 2000, 78, 1348.
34. Wool, R. P. Polymer Interfaces: Structure and Strength; Hanser Publishers; New York, 1995.
35. Wool, R. P.; Lu, J.; Can, E.; Thielemans, W.; Zhu, L.; Bonnaillie, L.; LaScala, J.; Hong, C.; Dweib, M.; McAninch, I.; Kulbick, A.; Hu, B.; Shenton, H. W., III. Bio-Based Composites; Proceedings of the European Congress on Composite Materials, ECCM-11; Rhodes, Greece, June 2, 2004.
36. Hong, C. K.; McChalicher, C. W. J.; Wool, R. P., to appear.
37. Bonnaillie, L.; Wool, R. P., to appear.
38. Wool, R. P.; Sun, X. S. Bio-Based Polymers and Composites; Elsevier: Boston, 2005.